Solar Energy Materials & Solar Cells 158 (2016) 37–42

Contents lists available at ScienceDirect

Solar Energy Materials & Solar Cells

journal homepage: www.elsevier.com/locate/solmat

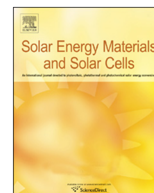

Extending the limits of screen-printed metallization of phosphorus- and boron-doped surfaces

Sabrina Werner*, Elmar Lohmüller, Andreas Wolf, Florian Clement

Fraunhofer Institute for Solar Energy Systems (ISE), Heidenhofstraße 2, 79110 Freiburg, Germany

ARTICLE INFO

Article history:
Received 28 March 2016
Received in revised form
29 May 2016
Accepted 30 May 2016
Available online 1 July 2016

Keywords:
Silicon solar cells
Specific contact resistance
Screen printing metallization
Phosphorus
Boron
Doping
Doping profile

ABSTRACT

This work demonstrates low-ohmic electrical contacting of phosphorus- and boron-doped surfaces (textured and passivated) with maximum dopant concentrations of only $N_{max} \approx 2 \cdot 10^{19}\ cm^{-3}$ by screen-printed and fired metallization. The achieved results using commercially available metallization pastes allow for a substantial extension of the limits in which screen-printed and fired metallization can be applied for solar cell fabrication. Despite the very low N_{max}, the investigations reveal reasonably low specific contact resistances of $\rho_C = (8 \pm 3)\ m\Omega\ cm^2$ for a silver paste on alkaline textured, phosphorus-doped, and SiN_x passivated surfaces, and $\rho_C = (3.7 \pm 0.7)\ m\Omega\ cm^2$ for a silver aluminum paste on alkaline textured, boron-doped, and Al_2O_3/SiN_x passivated surfaces.

© 2016 Elsevier B.V. All rights reserved.

1. Introduction

Tube furnace diffusion is currently the dominating technology to form highly doped regions in silicon solar cells. Utilizing phosphorus oxychloride ($POCl_3$) or boron tribromide (BBr_3) as liquid dopant precursors, this technology enables the formation of the highly doped regions for both p-type and n-type silicon solar cells. The optimization of diffusion processes and the resulting doping profiles are essential for further increasing the energy conversion efficiency of silicon solar cells. An approach to achieve higher open-circuit voltages V_{OC} is the reduction of the recombination parameter $j_{0,pass}$ of the passivated diffused surfaces. As a means of achieving this, the reduction of the maximum doping concentration N_{max} by e.g. in-situ oxidation proves to be very promising [1]. However, for the use of such improved doping profiles in cell technology in combination with screen-printed and fired metallization, a sufficiently low specific contact resistance ρ_C must be ensured. Moreover, the impact of the reduced peak doping on the dark saturation current densities $j_{0,met}$ underneath the metal contacts needs to be considered as well. The dynamic progress of screen-printing silver pastes in recent years enabled the electrical contacting of phosphorus-doped surfaces with $N_{max} \approx 2 \cdot 10^{20}\ cm^{-3}$ with low $1\ m\Omega\ cm^2 < \rho_C < 6\ m\Omega\ cm^2$ [2–4]. In this work, we demonstrate the low-ohmic electrical contacting of both phosphorus- and boron-doped surfaces (alkaline textured and passivated) by screen-printed and fired contacts for which N_{max} is reduced by one order of magnitude to $N_{max} \approx 2 \cdot 10^{19}\ cm^{-3}$.

2. Specific contact resistance: theory and state of the art

2.1. Models for current transport mechanisms

Depending on charge carrier concentration N and temperature T, different current transport models via charge carrier (tunneling) flow have been proposed for metal-semiconductor contacts [5–8] (the following stated values for N refer to room temperature $T = 300$ K, and serve as a rough reference point):

- Thermionic emission (TE) for low doping densities ($N < 10^{18}\ cm^{-3}$),
- Thermionic field emission (TFE) for medium doping densities ($10^{18}\ cm^{-3} \le N < 10^{20}\ cm^{-3}$), and
- Field emission (FE) for high doping densities ($N \ge 10^{20}\ cm^{-3}$).

The respective formulae to calculate the specific contact resistance ρ_C for each of these three current transport mechanisms can be found, e.g., in Ref. [9]. For the subsequent calculations of the theoretical dependence of ρ_C on N in this paper, the unified model from Varahramyan and Verret [8] is used. This unified model

* Corresponding author.
E-mail addresses: sabrina.werner@ise.fraunhofer.de (S. Werner), elmar.lohmueller@ise.fraunhofer.de (E. Lohmüller), andreas.wolf@ise.fraunhofer.de (A. Wolf), florian.clement@ise.fraunhofer.de (F. Clement).

http://dx.doi.org/10.1016/j.solmat.2016.05.064
0927-0248/© 2016 Elsevier B.V. All rights reserved.

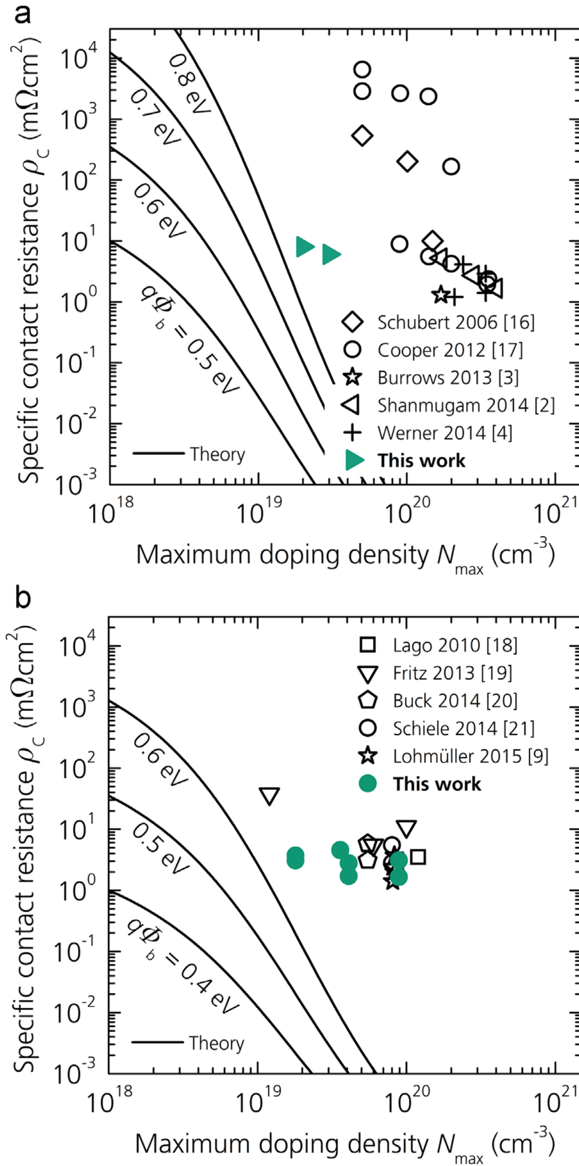

Fig. 1. Literature data (open symbols) for experimentally derived specific contact resistance ρ_C on (a) n-doped silicon and (b) p-doped silicon as function of the maximum doping density N_{max}. Type of metal contacts: (a) Ag and (b) AgAl. The theoretical curves (lines) are calculated according to Eqs. (1)–(3) considering the input parameters given in Table 1. The measured ρ_C of this work (filled symbols) demonstrate the extension of the limits for screen-printed and fired metallization towards lower N_{max}.

combines the TFE and FE tunneling mechanisms and reads

$$\rho_C(\text{TFE/FE}) = \bar{c}\frac{k_B}{qA^*T}\exp\left(\frac{q\phi_b'}{E_0}\right), \tag{1}$$

with the doping-type dependent constant $\bar{c}$, the Boltzmann constant k_B, the elementary charge q, the effective Richardson constant A^*, the effective Schottky barrier height[1] $q\phi_b'$, and the tunneling energy [5].

$$E_0 = E_{00}\cdot\coth\left(\frac{E_{00}}{k_BT}\right), \tag{2}$$

while E_{00} is another characteristic energy [5].

[1] In literature, both $q\phi'_b$ (in eV) and ϕ'_b (in V) are referred to as the effective Schottky barrier height.

Table 1
Overview of the parameters used within this paper for the theoretical calculation of ρ_C in dependence of N for both silicon doping types.

Parameter	$\bar{c}$	A^*	T	m_t^*/m_0	ε_r
(Unit)	(1)	(A cm^{-2} K^{-2})	(K)	(1)	(1)
n-type Si	0.425 [8]	112 [12]	300	0.3 [13]	11.7 [14]
p-type Si	0.355 [8]	32 [12]		0.4 [15]	

$$E_{00} = \frac{q\hbar}{2}\sqrt{\frac{N}{m_t^*\varepsilon_r\varepsilon_0}}, \tag{3}$$

with the reduced Plank's constant $\hbar$, the effective charge carrier tunneling mass m_t*(given as fraction of the electron mass m_0), the dielectric constant of silicon ε_r, and the permittivity of the vacuum ε_0.

For the calculations of the theoretical curves illustrated in Fig. 1 according to Eq. (1), the Schottky barrier height $q\phi_b$ is varied, while the other (doping type dependent) quantities are employed as summarized in Table 1. The effective Schottky barrier height $q\phi_b'$ calculates from the Schottky barrier height $q\phi_b$ considering image forces; see Eq. (9) in Ref. [9] or Refs. [10,11]. For silver contacts on phosphorus-doped surfaces a Schottky barrier height in the range of $q\phi_b$=0.78 eV is expected [10], for boron-doped surfaces $q\phi_b$=0.54 eV [10].

2.2. State of the art: specific contact resistances for screen-printed and fired metal contacts

The open symbols in Fig. 1 illustrate the state of the art ρ_C values for screen-printed and fired contact metallization on (a) phosphorus- and (b) boron-doped surfaces in dependence of N_{max} prior to this work [2–4,9,16–21]. For phosphorus doping profiles with $N_{max} \approx 2 \cdot 10^{20}$ cm^{-3}, low ρ_C values with 1 mΩ cm^2 < ρ_C < 6 mΩ cm^2 have been reported for screen-printed and fired silver contacts, while ρ_C increases significantly to several hundred mΩ cm^2 for $N_{max} \approx 5 \cdot 10^{19}$ cm^{-3}. On the other hand, low ρ_C values with 3 mΩ cm^2 < ρ_C < 6 mΩ cm^2 have been reported for boron doping profiles with $N_{max} \approx 6 \cdot 10^{19}$ cm^{-3} contacted with screen-printed and fired silver aluminum (AgAl) contacts. Again, ρ_C increases significantly for $N_{max} \approx 1 \cdot 10^{19}$ cm^{-3}.

Apparent from Fig. 1, a gap between experimental data and theoretical limit is present. A part of this gap originates from the fact that most screen-printed contacts only partially penetrate the dielectric passivation to an amount of a few percent and thus the macroscopic/effective specific contact resistance is strongly increased compared to the microscopic value that refers to the actual contact surface.

It will be briefly discussed why we choose to use N_{max} to quantify the doping concentration of interest for both doping types instead of the doping density directly at the silicon surface N_{surf}. For Ag pastes and phosphorus doping it is known that during the contact firing process—in case the current conduction to the phosphorus-doped silicon surface is mediated by metal crystallites—only small crystallites of a few 10 nm are formed [22–24]. Hence, the phosphorus doping concentration directly at the surface N_{surf} is of most interest. Note that phosphorus doping profiles do not feature a doping depletion zone towards the surface, since the solubility of phosphorus is higher in silicon than in silicon dioxide [25] (see also Fig. 2). Thus, N_{max} is equal to N_{surf} for phosphorus doping profiles. The situation is different for boron doping profiles; here the AgAl contacts form deep metal crystallites penetrating into the silicon surface up to depths of several microns [9,18,19,26]. Therefore, and as there is very often a doping

Download English Version:

https://daneshyari.com/en/article/6457416

Download Persian Version:

https://daneshyari.com/article/6457416

Daneshyari.com